Forward hadron productions in high energy *pp* collisions from a Monte-Carlo generator for color glass condensate

Wei-Tian Deng,[1] Hirotsugu Fujii,[2] Kazunori Itakura,[3,4] and Yasushi Nara[5]

[1]*School of Physics, Huazhong University of Science and Technology, Wuhan 430074, China*
[2]*Institute of Physics, University of Tokyo, Tokyo 153-8902, Japan*
[3]*KEK Theory Center, IPNS, KEK, Tsukuba 305-0801, Japan*
[4]*Department of Particle and Nuclear Studies, Graduate University for Advanced Studies(SOKENDAI), Tsukuba 305-0801, Japan*
[5]*Akita International University, Yuwa, Akita-city 010-1292, Japan*

(Received 16 October 2014; published 6 January 2015)

We develop a Monte Carlo event generator based on the combination of a parton production formula including the effects of parton saturation (called the DHJ formula) and a hadronization process due to the Lund string fragmentation model. This event generator is designed for the description of hadron productions at forward rapidities and in a wide transverse momentum range in high-energy proton-proton collisions. We analyze transverse momentum spectra of charged hadrons as well as identified particles, including pion, kaon, and (anti)proton at RHIC energy and ultraforward neutral pion spectra from the LHCf experiment. We compare our results to those obtained in other models based on parton-hadron duality and fragmentation functions.

DOI: 10.1103/PhysRevD.91.014006 PACS numbers: 24.85.+p, 12.38.Mh, 25.75.-q

I. INTRODUCTION

Theoretical understanding of hadron production in high-energy hadronic interactions is one of the most relevant subjects in QCD. For example, in ultrarelativistic heavy-ion collisions, the subsequent space-time evolution of a quark-gluon plasma (QGP) is described by relativistic hydrodynamics [1]. Thus, it is very important to fix a reliable initial condition for hydrodynamical simulations in order to extract the correct dynamics of the reaction. Another example is the air-shower development induced by ultra-high-energy cosmic rays, which is very sensitive to high-energy hadronic interactions [2]. The interactions are usually simulated using a Monte Carlo event generator, and the choice of an interaction model may critically affect the air shower analysis.

As an incident energy increases in a hadronic collision, reactions involving small Bjorken-x gluons become dominant, and a framework which treats a highly dense gluonic system is needed. The color glass condensate (CGC) framework has been proposed in order to describe such a dense gluon system [3,4] in which the saturation scale Q_s characterizes the nonlinear nature of the system.

For practical computation of gluon production in the CGC framework, two different approaches are often taken: solving the classical Yang-Mills equation on the lattice [5–7] or the k_T-factorized production formula with unintegrated gluon distribution (uGD) with saturation [8]. They have been successful in explaining many experimental data at RHIC and LHC energies. The models based on the k_T-factorization formula, such as the KLN model given in Ref. [9] and its extensions [10–13], describe hadron multiplicity distributions and transverse momentum (p_T) distributions in the low-momentum region under the assumption of local parton-hadron duality (LPHD) [14]. On the other hand, in the high-momentum region, it can be well reproduced by the k_T-factorization formula combined with the fragmentation functions [15–20].

A hybrid formalism was proposed in Ref. [21] to describe the collisions between a dilute projectile and a dense target (Dumitru-Hayashigaki-Jalilian-Marian (DHJ) formula). It has been applied to the computations of forward particle production spectra, not only for charged hadrons and pions but also for baryons [22] in d + Au collisions. The DHJ formula was also utilized to compute baryon productions for Au + Au collisions in Refs. [23,24], and it is found that transverse momentum spectra and net-baryon rapidity distributions in Au + Au collisions at RHIC are well described with the DHJ formula.

Substantial progress was made recently: the Balitsky-Kovchegov equation with running-coupling accuracy (rcBK equation) [25] was obtained, and numerical methods have been developed to solve the rcBK evolution [26]. A global analysis was performed with the rcBK equation for the nucleon structure function measured at HERA at small values of $x \leq 0.01$, which yields good fits (the AAMQS parametrization) [27]. At the same time, when applied to hadronic interactions, the AAMQS parametrization provides a good agreement with the data at RHIC and LHC [16–20]. For a recent review, see Ref. [28]. The next-to-leading-order (NLO) corrections to the hybrid formula were computed in Ref. [29] (See also [30]). It is found that the NLO corrections yield the same p_T dependence as the leading-order (LO) expression in the regime $p_T \leq Q_s$,

where nonlinear effects are strong, and thus the LO formula can be applied with a constant K factor at forward rapidities.

Geometrical fluctuations of the projectile and the target are important in nucleus-nucleus collisions. They are included in the k_T-factorization approach within a Monte Carlo–based formulation [19,31,32] and, this approach has been extensively used as initial conditions for the subsequent hydrodynamical evolution of a system [33–35]. However, it only provides the (energy) density distribution at each grid. Full event generation of all particles with their four-momenta assigned has not yet been implemented along this approach.

The first attempt to generate full parton configurations based on the KLN k_T factorization formula was done in Ref. [36] (BBL Monte Carlo model), and it was applied to high-energy cosmic ray air shower simulations. In BBL, momenta of quarks and gluons are generated according to the k_T-factorization formula, and the hadronization is performed using the Lund string fragmentation model. This approach allows one to describe particle production from the low- to high-momentum region consistently. They showed that atmospheric air showers are sensitive to the interactions with partons at very small x.

In this paper, we present a newly developed Monte Carlo event generator based on the DHJ formula which implements the latest theoretical update of the uGD function from the numerical solution of the rcBK equation. Specifically, we generate partons according to the DHJ formula together with initial and final state radiations based on the DGLAP evolution equation. Strings are formed by those produced partons and remnants that are fragmented into hadrons by the Lund string fragmentation model. We will compare our results to the forward hadron spectra in proton-proton collisions observed at the RHIC and LHCf experiments and discuss the mechanism of the particle production. Results with the LPHD and fragmentation function adopted to the DHJ formula are shown for comparison with our Monte Carlo approach.

This paper is organized as follows. In Sec. II, implementation of the DHJ formula into the Monte Carlo generator is explained. In Sec. III, we compare our numerical results to the transverse momentum distribution in proton-proton collisions at RHIC and LHC in forward rapidity regions. Results from different approaches are also shown for comparison. A summary is given in Sec. IV.

II. THE DHJ + LUND MODEL

We consider high-energy proton-proton scatterings at forward rapidities. We shall employ the DHJ hybrid formalism where we treat the collision between a large-x_1 [$= (p_T/\sqrt{s})\exp(y)$] parton (quarks or gluons) from the projectile and a small-x_2 [$= (p_T/\sqrt{s})\exp(-y)$] gluon from the target. Then the forward parton production cross section with transverse momentum p_T and rapidity y is given as

$$\frac{d\sigma_{\rm DHJ}}{dyd^2p_T} = \frac{K}{(2\pi)^2}\frac{\sigma_0}{2}\sum_{i=q,g} x_1 f_{i/p}(x_1,Q^2)N_i(x_2,p_T), \quad (1)$$

where $f_{i/p}$ is the collinear parton distribution function (PDF) for a large-x_1 parton i and N_i $(i = F, A)$ is the Fourier transform of the dipole scattering amplitude in the fundamental (for quark or antiquark scattering) or adjoint (for gluon scattering) representation for a small-x_2 gluon. We use $Q = p_T$ as a factorization scale for the PDF as a default value for the DHJ + Lund model. As a default setting in our model, the CTEQ5L [37] for the PDF and K factor of $K = 1.0$ are used. The average transverse area of the proton $\sigma_0/2 = 16.5$ mb is obtained by the DIS fits at HERA [20,27]. The uGD functions $N_{F,A}$ are obtained as the numerical solution of the rcBK equation and are fitted to the HERA data [27]. Specifically, the parameter set g1.101 in Ref. [19] is used in this paper in which the initial condition for N_F in the coordinate representation at $x_0 = 0.01$ is taken to be

$$N_F(r,x_0) = 1 - \exp\left[-\frac{(r^2Q_{s0}^2)^\gamma}{4}\ln\left(\frac{1}{\Lambda r}+e\right)\right], \quad (2)$$

where r is the transverse size of a color dipole, $\gamma = 1.101$, $Q_{s0}^2 = 0.157$ GeV^2, $\Lambda = 0.241$ GeV, and we assume the impact parameter independent rcBK equation.

In Fig. 1, a schematic picture of what the DHJ + Lund model simulates is illustrated for $gg \to g$ together with the initial and final state radiations. Gluons and quarks are generated randomly according to the formula Eq. (1) with the minimum momentum $p_{T,\rm min} = 1$ GeV. We have checked that the transverse momentum distribution is insensitive to $p_{T,\rm min}$. Simulations with $p_{T,\rm min} = 0.25$ GeV yield similar results as $p_{T,\rm min} = 1$ GeV, which will be presented in this paper. Initial radiations for the high-x projectile part and final state radiations are included in line with the PYTHIA approach [38,39], but explicit gluon

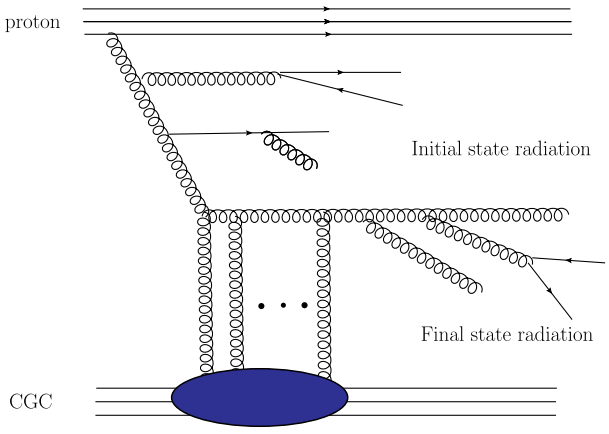

FIG. 1 (color online). Schematic picture of a possible event in which a interaction $gg \to g$ with initial and final state radiations is simulated by the DHJ + Lund model.

productions from the initial state radiation due to x evolution are not included in this work.

The effects of multiple parton interaction (MPI) are simulated based on the eikonal model [40], which is used in several event generators such as HIJING [41–43], SIBYLL [44,45], and HERWIG++ [46,47]. By assuming that each interaction is independent, the probability of n scattering is given by

$$P_n = \frac{n(b,s)^n}{n!}\exp(-n(b,s)), \tag{3}$$

where

$$n(b,s) = A(b)\sigma_{\mathrm{DHJ}}(s) \tag{4}$$

is the average number of partonic collisions at a given impact parameter b with the invariant mass of the collision s. $A(b)$ is the spatial overlap of the two colliding hadrons, and we take the Gaussian form,

$$A(b) = \frac{1}{4\pi B}\exp\left(-\frac{b^2}{4B}\right), \tag{5}$$

with the parameter $B = 0.25$ fm^2. Notice that the multiple scattering of an incoming parton with a coherent color field in the target CGC is already included in σ_{DHJ}. MPI describes events that include several hard scatterings. In an event with several interactions, we will have several hard scatterings of the types $gg \to g$ or $qg \to q$. Among several hard scatterings, quark production from the $qg \to q$ process is generated only once, if it is selected, and the rest of all interactions are assumed to be $gg \to g$ scattering for simplicity. More sophisticated implementation of multiple parton interaction will be discussed elsewhere.

We need to introduce hadronization of the parton in order to compare it with experimentally measured hadrons. The hadronization process is an entirely nonperturbative process, and we have only phenomenological approaches. The hypothesis of LPHD [14] has been formulated based on the observation that parton distribution computed in the perturbative QCD (pQCD) approach gives a good description of hadrons even at small p_T. On the other hand, the fragmentation function is used to hadronize the partonic system above the factorization scale. The Lund string model of hadronization has been developed based on the massless relativistic string as a model for the QCD color field [48] and implemented in the Monte Carlo event generator PYTHIA [38]. In this paper, we utilize the Lund model for the hadronization.

Besides hard scatterings between the two hadrons, soft interactions are modeled by the excitations of two strings. It is generated with the fractional energy x of the quark, which is chosen according to the probability profile

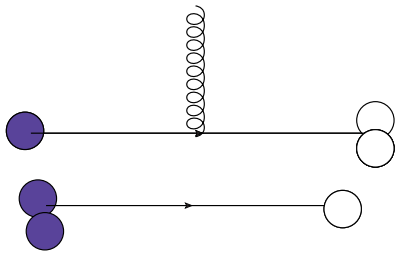

FIG. 2 (color online). Schematic picture of a possible string configuration after the collision, where two strings are formed and stretched between quarks and diquarks. The gluon which is produced in the $gg \to g$ process is attached to one of the strings.

$$P(x) = \frac{(1-x)^\alpha}{\sqrt[4]{x^2 + c/s}}, \tag{6}$$

with the default parameter in PYTHIA6 [38]: $\alpha = 3$ and $c = 0.36$. We use PYTHIA8.186 [49] to simulate the string fragmentation into hadrons. A simplest string configuration in a Monte Carlo event in our model is depicted in Fig. 2. When one $gg \to g$ interaction occurs and there is no radiation, there are two strings formed, one of which will have one gluon attached. There are, of course, many other string configurations in the simulation, although we do not show all of them here.

III. COMPARISON WITH THE EXPERIMENTAL DATA

In this section, we compare our results to the experimental data at both RHIC and LHC energies. Within the DHJ + Lund model, we have generated 70 million events at RHIC energy, and 1 million events at LHC energy, which were then used to compute the transverse momentum distributions of the produced hadrons in pp collisions.

For other model approaches, we present the results of the DHJ formulation with the LPHD ansatz (DHJ + LPHD) in the low-momentum region and those of the DHJ formulation with fragmentation function (DHJ + FF) in the high-momentum region. We use CTEQ5L (LO) [37] for the PDF and DSS LO fragmentation function [50] for FF. We also compare PYTHIA and HIJING results in which both soft and pQCD mini-jet productions are included.

A. Charged hadrons

For later discussions, let us first explain the DHJ + LPHD model briefly. We basically follow the same approach as in Ref. [12]: Transverse momentum of the parton q_T is obtained by $q_T = p_T/\langle z\rangle$ in Eq. (1), and q_T is replaced by $m_T = \sqrt{q_T^2 + m_{\mathrm{jet}}^2}$ in order to take into account mass effect. In the framework of the LPHD in Ref. [12], $\langle z\rangle \approx 0.5$ was used and good agreement with the data was obtained for the transverse momentum distributions for charged hadrons at low transverse momentum range less

than 4 GeV at midrapidity at $\sqrt{s} = 2.36$ TeV. Thus, in the case of the forward rapidity y region, we take an average of z value as

$$\langle z \rangle = \frac{(1 + z_{\min})}{2} = \frac{1 + \frac{m_T}{\sqrt{s}} e^y}{2}. \tag{7}$$

The saturation scale Q_s is used for the factorization scale in the PDF.

In Fig. 3, transverse momentum distributions for negatively charged hadrons in pp collisions at $\sqrt{s} = 200$ GeV at rapidity 2.2 and 2.3 from the DHJ + LPHD model are shown together with the experimental data from BRAHMS [51]. As an overall normalization, we used a K factor of 2.5. We have checked that the results in Fig. 3 are not sensitive to the value of the mass of the mini-jet $m_{\rm jet}$ in the range from $m_{\rm jet} = 0.0$ to 0.5 GeV. It is remarkable that under the assumption of LPHD, the DHJ framework works in the low-momentum region for the description of transverse momentum distributions even though it is not legitimate to use PDF in such a low p_T range. However, the LPHD approach does not work in the high-momentum region. Instead, the fragmentation of the produced parton into hadrons will be the appropriate picture there. Indeed, the results of the DHJ formula convoluted with the DSS LO fragmentation function [50] describe the data in the high-momentum region as shown in Fig. 3. The factorization scale dependence is also checked, and it is found that the results for $Q = p_T$ are twice as large as the one for $Q = 2p_T$ with almost the same p_T slope, where $K = 2.5$ is used in the plot. Thus, scale dependence can be absorbed by changing the K factor. See also Refs. [16–20] for the CGC predictions for forward hadron productions with fragmentation functions.

We now turn to the Monte Carlo event generator DHJ + Lund results. Figure 4 shows the negatively charged hadron spectra and neutral pion in pp collisions at $\sqrt{s} = 200$ GeV obtained by the DHJ + Lund model, together with the BRAHMS data [51] and PHENIX data [52]. In the DHJ + Lund approach, hadron spectra from the low- to high-momentum region can be described within a single framework. Note that we do not need intrinsic k_T to fit the data, which is often introduced in the conventional pQCD-based models. In the DHJ + LPHD approach, the spectrum in the low-momentum region is entirely described by the soft gluons, but in the DHJ + Lund approach, it is modeled by the string fragmentation.

It would be informative to see the results from a model based on the conventional collinear factorization of pQCD. For this purpose, we plot HIJING results in Fig. 4, which we call HIJING2D since it is a modified version from the original HIJING2.0 [43]. In HIJING, the nucleon-nucleon inelastic cross section is given by the eikonal formalism,

$$\sigma_{\rm in} = \int_0^\infty d^2b[1 - e^{2\chi(b,s)}], \tag{8}$$

where the eikonal function $\chi(b, s)$ at an impact parameter b and at the invariant mass s is obtained as the sum of the

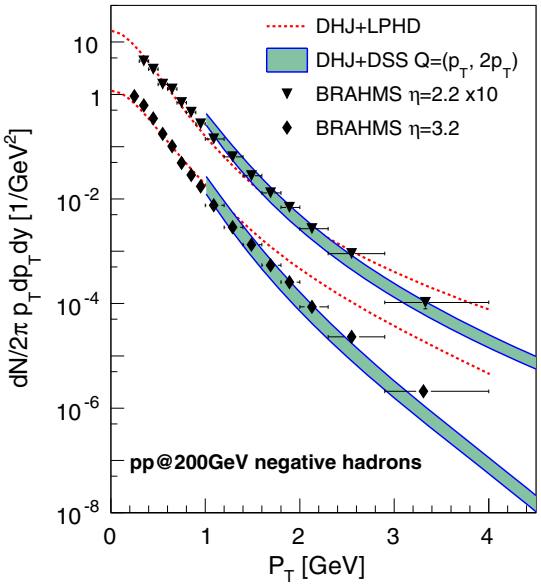

FIG. 3 (color online). Negatively charged hadron transverse momentum distributions in pp collisions at $\sqrt{s} = 200$ GeV at $y = 2.2$ and 3.2 from the BRAHMS experiment [51] are compared with the DHJ + LPHD model and DHJ + DSS independent fragmentation. $K = 2.5$ is used for both calculations. In the DHJ + DSS results, scale dependence between $Q = p_T$ and $Q = 2p_T$ is shown by the width of the band.

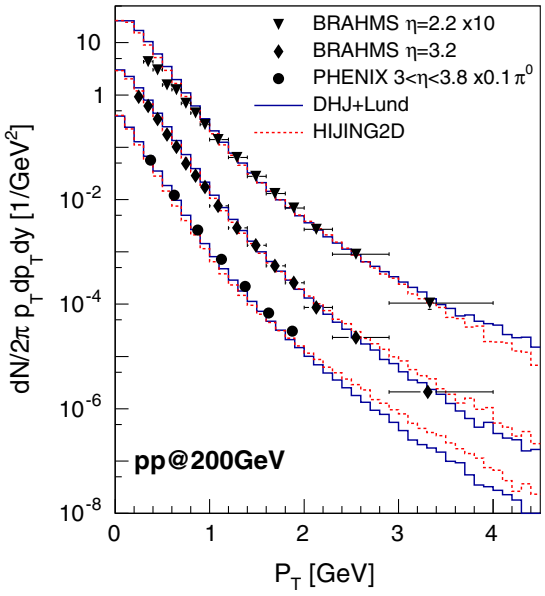

FIG. 4 (color online). Negatively charged hadron spectra and neutral pion spectra in pp collisions at $\sqrt{s} = 200$ GeV. Data are from the BRAHMS [51] and PHENIX [52]. Results from DHJ + Lund (solid lines) and HIJING2D(dotted lines) are compared.

pQCD $2 \to 2$ cross sections and the soft parton-parton collisions,

$$\chi(b,s) = \frac{1}{2}[\sigma_{\rm jet} T(b) + \sigma_{\rm soft} T(b)], \tag{9}$$

where $T(b)$ is the nucleon-nucleon overlap function and is taken to be (the Fourier transform of) the dipole form factor. The LO pQCD $2 \to 2$ jet cross section in pp collisions at $\sqrt{s} = 200$ GeV is calculated with CTEQ6M PDF [53] and the K factor of 2.5, assuming the p_T cutoff $p_0 = 2.1$ GeV. In HIJING2D, $\sigma_{\rm soft} = 58$ mb is used to fit the total pp cross section and pseudorapidity distribution for charged hadrons in pp collisions at $\sqrt{s} = 200$ GeV. The original HIJING model switches off the option for the popcorn model [54] in the Lund string fragmentation, and the leading diquark does not break there. But it is switched on in HIJING2D. HIJING2D results, shown in Fig. 4, also describe the experimental data very well. This means that we do not see any distinct effects of CGC in the charged hadron data of BRAHMS and neural pion data of PHENIX in pp collisions at $\sqrt{s} = 200$ GeV. This fact is actually encouraging: If one wants to construct a model in which both CGC and pQCD processes are included, it is expected that the transition from the pQCD to CGC description will be smooth.

We also compare the neutral pion momentum distributions in pp collisions at forward rapidities from the STAR experiments [55] in Fig. 5. The DHJ + Lund model overestimates the data by a factor of 2, although the slope is close to the data. We note that DHJ + Lund is consistent with the DHJ + DSS approach ($K = 2.5$). On the other hand, HIJING2D overestimates all data, and its slopes are much harder than the data. In the low-momentum region $p_T < 1$ GeV, both DHJ + Lund and HIJING2D model predictions are consistent with each other for all rapidities. It is seen that there is a significant difference between HIJING2D and DHJ + Lund approaches at momenta larger than 1 or 2 GeV. The slopes in the HIJING2D results are much harder than those of the DHJ + Lund model results, which are more clearly seen at larger rapidity. We have checked that PYTHIA6 gives quite similar results as HIJING2D, but PYTHIA8.1 results are very close to the DHJ + Lund model results as shown in Fig. 5. In Ref. [55], it was reported that NLO pQCD calculations agree with the forward neutral pion from pp collisions, despite that its spectrum is not consistent with the data for d + Au collisions.

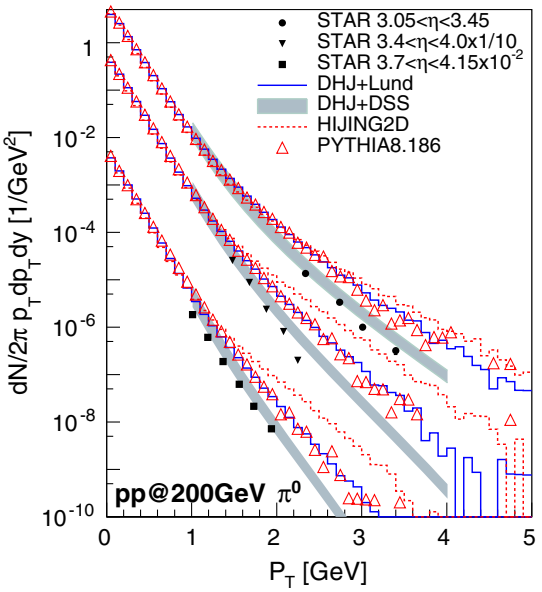

FIG. 5 (color online). Neutral pion invariant cross sections from STAR [55] in pp collisions at $\sqrt{s} = 200$ GeV are compared to the DHJ + Lund model (solid lines), HIJING2D (dotted lines), PYTHIA8.1 (triangles), and DHJ + DSS (bands). The DHJ + DSS results are for $K = 2.5$ and $Q = (p_T, 2p_T)$. All theoretical results are obtained by averaging over the given rapidity bin.

B. Identified hadrons

We turn now to the comparison of identified hadron spectra at forward rapidities. In Fig. 6, transverse momentum distributions for pion, kaons, protons, and antiprotons from pp collisions at $\sqrt{s} = 200$ GeV at rapidities $y = 2.95$ and $y = 3.3$ [56] are compared with the DHJ + Lund model results. Our model reasonably describes the BRAHMS data in the low-momentum region $p_T < 2$ GeV, but slopes are flatter at high p_T. It should be noted that the DHJ + Lund model describes the proton and antiproton yields simultaneously. DHJ + DSS results for $Q = p_T$ and $Q = 2p_T$ with $K = 2.5$ are also shown in Fig. 6. The agreement with the BRAHMS data is reasonably good for pions and kaons. However, the proton yield in DHJ + DSS is below the data by a factor of 2 and 5 for rapidities $y = 2.95$ and $y = 3.3$, respectively. On the other hand, antiproton yields are bigger by a factor of 2 in DHD + DSS.

The DHJ + FF approach was applied to compute the proton yield in d + Au collisions at $\sqrt{s} = 200$ GeV in Ref. [22]. The fragmentation function extracted from the Lund string model [57] scaled by the AKK fragmentation function [58] was used in the calculations. It is pointed out that the contributions from diquark fragmentation play an essential role in the forward baryon production. Note that both the DHJ + Lund model and HIJING2D take into account these diquark contributions. Thus, we expect that proton spectra in the DHJ + DSS approach also can be improved by taking such effects into account.

Various model predictions for the proton distribution at $y = 3.3$ are compared in Fig. 7. DHJ + DSS with $K = 7$ and $Q = p_T$ reproduces the proton data very well, although this value of the K factor is inconsistent with pion and kaon data. We find that HIJING2D yields the same result as PYTHIA6, and both show much flatter proton distribution

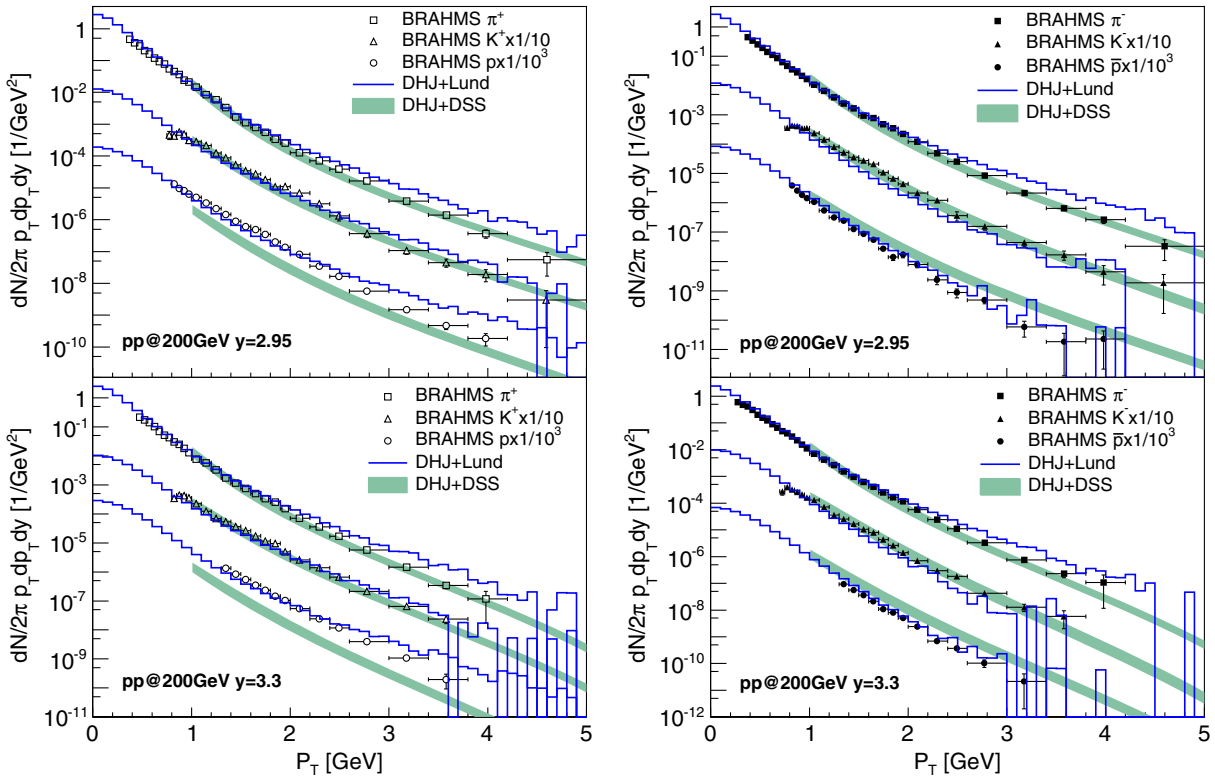

FIG. 6 (color online). Inclusive pions, kaons, protons, and antiprotons transverse momentum distributions in pp collisions at $\sqrt{s} = 200$ GeV at rapidities $y = 2.95$ and $y = 3.3$ obtained by the DHJ + Lund model (solid line) and the DHJ + DSS (box). Positively (negatively) charged particles are shown in the left (right) panel. Data are from the BRAHMS Collaboration [56]. In the DHJ + DSS calculations, $K = 2.5$ is used, and the width of the bands indicates the different choice of the factorization scales within $Q = (p_T, 2p_T)$.

than the data. On the other hand, the slope of the DHJ + Lund model at $p_T < 3$ GeV is close to the data, although the high p_T part is flatter than the data, which is not seen in the results with the DSS fragmentation function. It is seen that the PYTHIA8.1 result is in quite good agreement with experimental data as shown in Fig. 7. Thus, it is hard to see the distinct CGC effects from the proton transverse momentum distribution in pp collisions at $\sqrt{s} = 200$ GeV.

Finally, we should remark on the NLO pQCD results. In Ref. [56], it is reported that NLO pQCD calculations describe the distribution of pions and kaons, but fail to fit the proton and antiproton yields at the same time.

C. LHCf data

In this section, we analyze neutral pion transverse spectra from the LHCf experiment [59] in pp collisions at $\sqrt{s} = 7$ TeV. Since measurement was performed in the very forward rapidity range $8.9 < y < 11.0$, the produced particles come from the extremely high-x_1 and low-x_2 regions of the PDF. In Ref. [60], LHCf data were analyzed based on the DHJ formula convoluted with the fragmentation function, and it was found that slopes are much steeper than the LHCf data.

First let us study the contributions of gluons and quarks from CGC to the LHCf data. In Fig. 8 we present the DHJ + LPHD results of the neutral pion transverse momentum spectra in pp collisions at $\sqrt{s} = 7$ TeV at different rapidities compared to LHCf data [59]. The factorization scale of the PDF is chosen to be $Q = Q_s$, where Q_s is a saturation scale. Sensitivities to the choice of the factorization scale of the PDF are also shown in Fig. 8 as a band between the results with $Q/2$ and $2Q$. We have checked the sensitivity of the particle spectra to the PDF. The calculations with GRV94L and CTEQ6M PDF yield results similar to the CTEQ5L results. DHJ + LPHD describes the correct slopes for most of the rapidity bins. However, we found that in order to fit the data, we need an extremely large $K = 22(15)$ factor assuming the inelastic (nondiffractive) cross section of $\sigma_{\rm inel} = 73.6$ mb [59] ($\sigma_{\rm nondif} = 48.45$ mb). (If we do not include the factor $\sigma_0/2$, the K factor will be $K = 5$). We conclude, therefore, that the DHJ + LPHD approach does not work for explaining the LHCf forward pion data.

We also test a different approach in which gluons from the DHJ formula fragment into hadrons independently. The results from the independent fragmentation are plotted by histogram in Fig. 8. For this hadronization process, the Lund model is also used. In this model, reasonable K

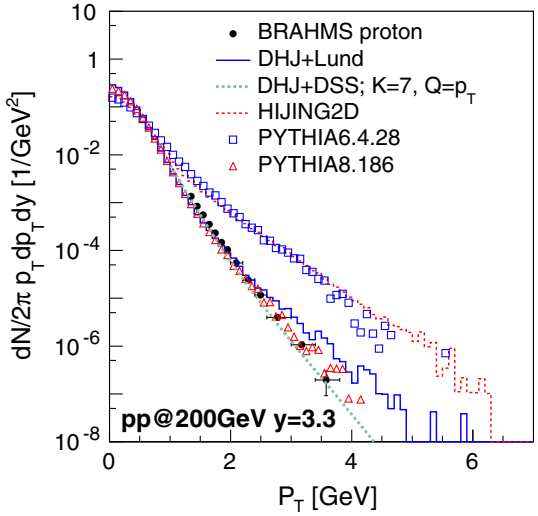

FIG. 7 (color online). Inclusive proton invariant cross sections in pp collisions at $\sqrt{s} = 200$ GeV at $y = 3.3$ are compared to the DHJ + LUND model (solid lines), HIJING2D (dashed lines), DHJ + DSS (dotted lines), PYTHIA6.4.28 (squares), and PYTHIA8.168 (triangles).

factor $K = 2.5$ is obtained to fit the data. It is interesting to see that the Lund independent fragmentation model describes the correct slopes. However, independent fragmentation picture may not be adequate to describe very low momentum hadrons.

Finally, the results of the DHJ + Lund model for neutral pion at $\sqrt{s} = 7$ TeV are shown in Fig. 9 together with the results in which only soft interactions are included. By the soft interaction, we mean that two strings are excited according to the formula (6), and possible additional string productions between sea quarks are neglected. Increase of the yield in the model with the soft interaction only may be understood as follows: In this model, strings are stretched almost parallel to the beam direction and are likely to produce pions in the forward region. On the other hand, forward pion production is suppressed by the gluons attached in the string when CGC gluons are included. The DHJ + Lund model agrees with the data at low momentum, and its slopes are slightly harder than the LHCf data. The effects of diffractive interactions are checked by PYTHIA6, and we find that single and double diffractive interactions yield similar results as the non-diffractive one, except the single-diffractive scattering in which one forward particle goes to the negative rapidity direction whose contribution is estimated at about 12% of the inelastic cross section. From our analysis, most of the neutral pions in the ultraforward region can be explained by the soft physics which come from the decay of strings.

As pointed out in Ref. [59], pion distribution is sensitive to the choice of the baryon production model. Indeed, we have checked that if the popcorn model [54] is switched off, much steeper spectra are obtained. which is inconsistent with the data.

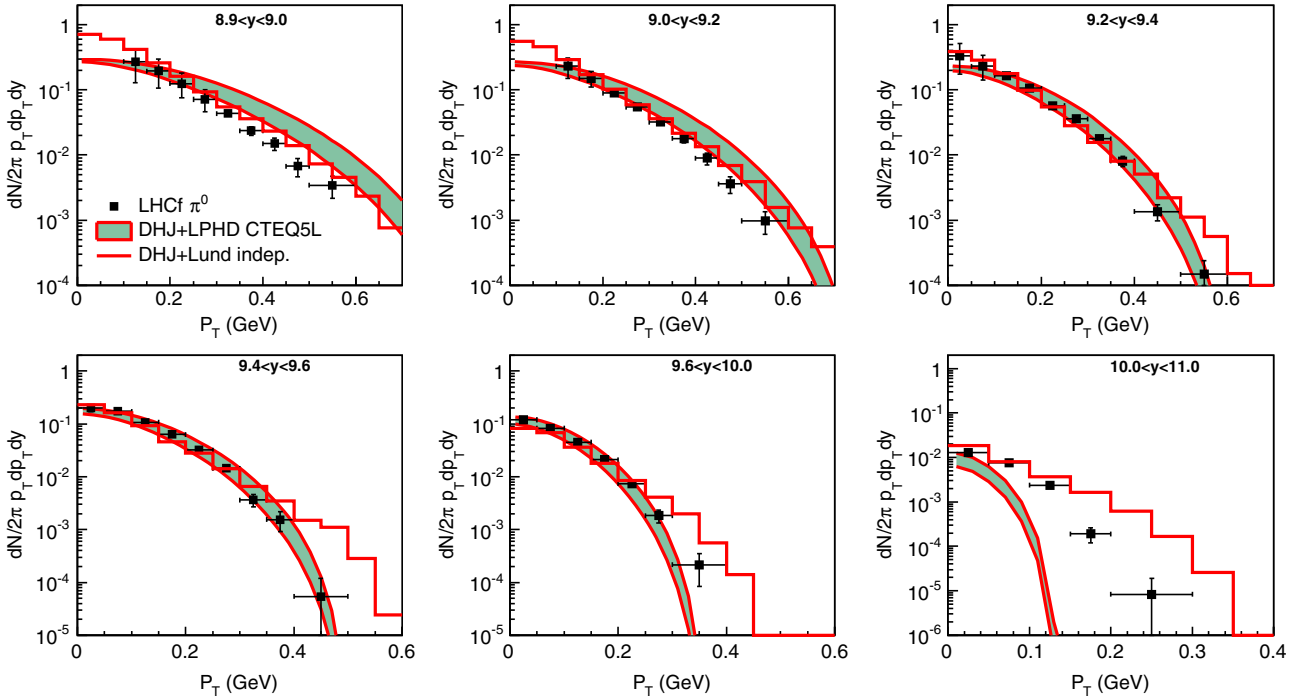

FIG. 8 (color online). Comparison of invariant cross sections for the neutral pion from LHCf in pp collisions at $\sqrt{s} = 7$ TeV with the DHJ + LPHD model and the DHJ with the independent fragmentation model of Lund.

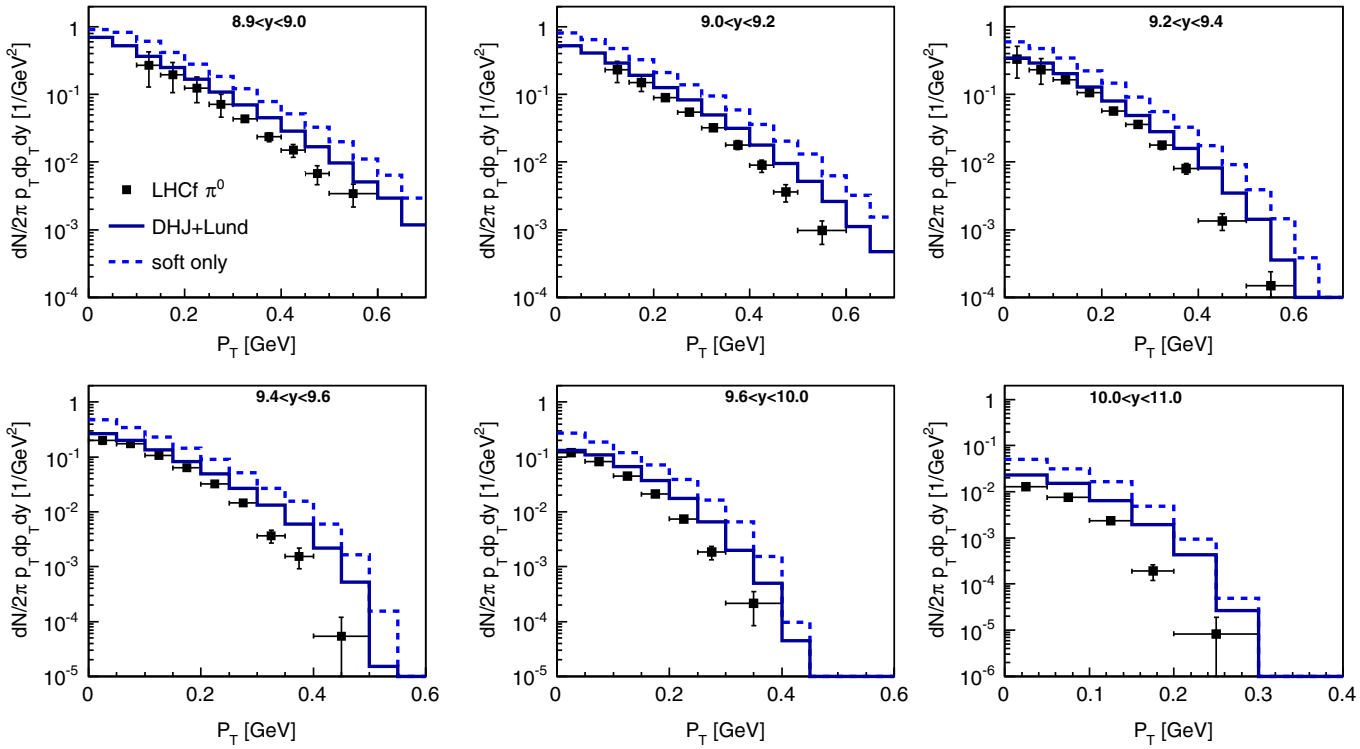

FIG. 9 (color online). Comparison of invariant cross sections for the neutral pion in pp collisions at $\sqrt{s} = 7$ TeV from the LHCf experiment [59] with the DHJ + Lund model (solid lines). The results, which only include the soft string excitations, are shown by the dashed lines.

It is reported from LHCf [61] that the nuclear modification factor of forward neutral pion in proton-lead collisions at $\sqrt{s_{NN}} = 5.02$ TeV exhibits strong suppression, and it increases with transverse momentum. However, the hadronic interaction model predictions show almost flat p_T dependence. It will be interesting to explore p-Pb collisions within our approach in the future.

IV. SUMMARY

In this paper, we have developed a Monte Carlo version of the DHJ formula (DHJ + Lund model) for proton-proton collisions. In this model, we explicitly generate $gg \to g$ and $gq \to q$ scatterings together with the initial and final state radiations. Those produced partons are connected with the remnant excited strings and decay into hadrons according to the Lund string fragmentation model.

We have compared the results of our model with hadron transverse momentum distributions at forward rapidities and from low- to high-momentum regions at both RHIC and LHC energies. We also studied the spectra for identified hadrons within our model. The model provides a unified description of the hadron spectra from the nonperturbative low- to high-momentum region. It is shown that the DHJ + Lund model yields results that are consistent with the approach with the fragmentation function for charged, pion, and kaon spectra in high-p_T regions. Some improved description of the baryon production at forward rapidities was seen.

We also analyzed LHCf ultraforward neutral pion spectra by both the DHJ + LPHD and DHJ + Lund models. We found that the LPHD approach, in which the hadron spectrum can be understood by the parton spectrum itself, is in agreement with the experimental slopes but requires a significantly large K factor to fit the LHCf data. On the other hand, the DHJ + Lund model agrees with the LHCf data at low momentum, even though its slopes are slightly harder than the data. The dominant process for such ultraforward pions in the DHJ + Lund model is the soft excitation of strings and their fragmentations. Therefore, the ultraforward neutral pions may be understood by the production due to nonperturbative soft physics.

In a future work, we are planning to extend the model to proton-nucleus and nucleus-nucleus collisions.

ACKNOWLEDGMENTS

Y. N. is thankful to Adrian Dumitru for useful comments. The authors thank K. Kasahara, H. Menjo, and T. Sako for providing the main program for PYTHIA8. This work was partially supported by a Grant-in-Aid for Scientific Research (B) (22340064).

[1] U. Heinz and R. Snellings, Annu. Rev. Nucl. Part. Sci. **63**, 123 (2013).
[2] R. Engel, D. Heck, and T. Pierog, Annu. Rev. Nucl. Part. Sci. **61**, 467 (2011).
[3] L. D. McLerran and R. Venugopalan, Phys. Rev. D **49**, 2233 (1994); **49**, 3352 (1994); **50**, 2225 (1994).
[4] F. Gelis, E. Iancu, J. Jalilian-Marian, and R. Venugopalan, Annu. Rev. Nucl. Part. Sci. **60**, 463 (2010).
[5] A. Krasnitz and R. Venugopalan, Nucl. Phys. **B557**, 237 (1999); A. Krasnitz, Y. Nara, and R. Venugopalan, Phys. Rev. Lett. **87**, 192302 (2001); , Nucl. Phys. **A727**, 427 (2003).
[6] T. Lappi, Phys. Rev. C 67 (**2003**) 054903; Eur. Phys. J. C **55**, 285 (2008); Phys. Lett. B **703**, 325 (2011).
[7] B. Schenke, P. Tribedy, and R. Venugopalan, Phys. Rev. Lett. **108**, 252301 (2012); Phys. Rev. C **86**, 034908 (2012); C. Gale, S. Jeon, B. Schenke, P. Tribedy, and R. Venugopalan, Phys. Rev. Lett. **110**, 012302 (2013); B. Schenke, P. Tribedy, and R. Venugopalan, Phys. Rev. C **89**, 024901 (2014).
[8] Y. V. Kovchegov and K. Tuchin, Phys. Rev. D **65**, 074026 (2002).
[9] D. Kharzeev and M. Nardi, Phys. Lett. B **507**, 121 (2001); D. Kharzeev and E. Levin, Phys. Lett. B **523**, 79 (2001); D. Kharzeev, E. Levin, and M. Nardi, Nucl. Phys. **A730**, 448 (2004); Phys. Rev. C **71**, 054903 (2005); Nucl. Phys. **A747**, 609 (2005); A. Dumitru, D. E. Kharzeev, E. M. Levin, and Y. Nara, Phys. Rev. C **85**, 044920 (2012).
[10] H. J. Drescher, A. Dumitru, A. Hayashigaki, and Y. Nara, Phys. Rev. C **74**, 044905 (2006).
[11] E. Levin and A. H. Rezaeian, Phys. Rev. D **82**, 054003 (2010).
[12] E. Levin and A. H. Rezaeian, Phys. Rev. D **82**, 014022 (2010).
[13] E. Levin and A. H. Rezaeian, Phys. Rev. D **83**, 114001 (2011).
[14] Ya. I. Azimov, Yu. L. Dokshitzer, V. A. Khoze, and S. I. Troyan, Z. Phys. C **27**, 65 (1985); **31**, 213 (1986).
[15] D. Kharzeev, Y. V. Kovchegov, and K. Tuchin, Phys. Lett. B **599**, 23 (2004).
[16] J. L. Albacete and C. Marquet, Phys. Lett. B **687**, 174 (2010).
[17] H. Fujii, K. Itakura, Y. Kitadono, and Y. Nara, J. Phys. G **38**, 124125 (2011).
[18] H. Fujii, K. Itakura, and Y. Nara, Prog. Theor. Phys. Suppl. **193**, 216 (2012).
[19] J. L. Albacete, A. Dumitru, H. Fujii, and Y. Nara, Nucl. Phys. **A897**, 1 (2013).
[20] T. Lappi and H. Mäntysaari, Phys. Rev. D **88**, 114020 (2013).
[21] A. Dumitru, A. Hayashigaki, and J. Jalilian-Marian, Nucl. Phys. **A765**, 464 (2006); **A770**, 57 (2006).
[22] A. Hayashigaki, Nucl. Phys. **A775**, 51 (2006).
[23] Y. Mehtar-Tani and G. Wolschin, Phys. Rev. C **80**, 054905 (2009).
[24] F. O. Duraes, A. V. Giannini, V. P. Goncalves, and F. S. Navarra, Phys. Rev. C **89**, 035205 (2014).
[25] I. Balitsky, Phys. Rev. D **75**, 014001 (2007); Y. V. Kovchegov and H. Weigert, Nucl. Phys. **A784**, 188 (2007); **A789**, 260 (2007).
[26] J. L. Albacete and Y. V. Kovchegov, Phys. Rev. D **75**, 125021 (2007).
[27] J. L. Albacete, N. Armesto, J. G. Milhano, P. Quiroga-Arias, and C. A. Salgado, Eur. Phys. J. C **71**, 1705 (2011); see also J. L. Albacete, N. Armesto, J. G. Milhano, and C. A. Salgado, Phys. Rev. D **80**, 034031 (2009).
[28] J. L. Albacete, A. Dumitru, and C. Marquet, Int. J. Mod. Phys. A **28**, 1340010 (2013).
[29] G. A. Chirilli, B.-W. Xiao, and F. Yuan, Phys. Rev. Lett. **108**, 122301 (2012); Phys. Rev. D **86**, 054005 (2012); A. M. Stasto, B.-W. Xiao, and D. Zaslavsky, Phys. Rev. Lett. **112**, 012302 (2014); A. M. Staśto, B. W. Xiao, F. Yuan, and D. Zaslavsky, Phys. Rev. D **90**, 014047 (2014).
[30] Z. B. Kang, I. Vitev, and H. Xing, Phys. Rev. Lett. **113**, 062002 (2014); B. W. Xiao and F. Yuan, arXiv:1407.6314.
[31] H.-J. Drescher and Y. Nara, Phys. Rev. C **75**, 034905 (2007); **76**, 041903(R) (2007).
[32] J. L. Albacete and A. Dumitru, arXiv:1011.5161; J. L. Albacete, A. Dumitru, and Y. Nara, J. Phys. Conf. Ser. **316**, 012011 (2011); Y. Nara, Prog. Theor. Phys. Suppl. **193**, 145 (2012); A. Dumitru and Y. Nara, Phys. Rev. C **85**, 034907 (2012).
[33] T. Hirano, P. Huovinen, K. Murase, and Y. Nara, Prog. Part. Nucl. Phys. **70**, 108 (2013); T. Hirano and Y. Nara, Prog. Theor. Exp. Phys. **2012**, 01A203 (2012).
[34] T. Hirano, P. Huovinen, and Y. Nara, Phys. Rev. C **83**, 021902 (2011); **84**, 011901 (2011).
[35] Z. Qiu, C. Shen, and U. Heinz, Phys. Lett. B **707**, 151 (2012); U. Heinz, Z. Qiu, and C. Shen, Phys. Rev. C **87**, 034913 (2013); H. Song, S. Bass, and U. W. Heinz, Phys. Rev. C **89**, 034919 (2014).
[36] H. J. Drescher, A. Dumitru, and M. Strikman, Phys. Rev. Lett. **94**, 231801 (2005); arXiv:hep-ph/0501165.
[37] H. L. Lai, J. Huston, S. Kuhlmann, J. Morfin, F. Olness, J. F. Owens, J. Pumplin, and W. K. Tung, Eur. Phys. J. C **12**, 375 (2000).
[38] T. Sjostrand, S. Mrenna, and P. Z. Skands, J. High Energy Phys. 05 (2006) 026.
[39] T. Sjöstrand, Comput. Phys. Commun. **82**, 74 (1994).
[40] J. M. Butterworth, J. R. Forshaw, and M. H. Seymour, Z. Phys. C **72**, 637 (1996); L. Durand and P. Hong, Phys. Rev. Lett. **58**, 303 (1987); L. Durand and H. Pi, Phys. Rev. D **40**, 1436 (1989).
[41] X. N. Wang and M. Gyulassy, Phys. Rev. D **44**, 3501 (1991).
[42] M. Gyulassy and X. N. Wang, Comput. Phys. Commun. **83**, 307 (1994).
[43] W. T. Deng, X. N. Wang, and R. Xu, Phys. Rev. C **83**, 014915 (2011).
[44] R. S. Fletcher, T. K. Gaisser, P. Lipari, and T. Stanev, Phys. Rev. D **50**, 5710 (1994).
[45] E. J. Ahn, R. Engel, T. K. Gaisser, P. Lipari, and T. Stanev, Phys. Rev. D **80**, 094003 (2009).
[46] M. Bahr, S. Gieseke, and M. H. Seymour, J. High Energy Phys. 07 (2008) 076.
[47] M. Bahr, S. Gieseke, M. A. Gigg, D. Grellscheid, K. Hamilton, O. Latunde-Dada, S. Platzer, P. Richardson *et al.*, Eur. Phys. J. C **58**, 639 (2008).
[48] B. Andersson, G. Gustafson, G. Ingelman, and T. Sjostrand, Phys. Rep. **97**, 31 (1983); B. Andersson, *The Lund*

Model (Cambridge University Press, Cambridge, England, 1998).
[49] T. Sjostrand, S. Mrenna, and P. Z. Skands, Comput. Phys. Commun. **178**, 852 (2008).
[50] D. de Florian, R. Sassot, and M. Stratmann, Phys. Rev. D **75**, 114010 (2007); **76**, 074033 (2007).
[51] I. Arsene *et al.* (BRAHMS Collaboration), Phys. Rev. Lett. **93**, 242303 (2004).
[52] A. Adare *et al.* (PHENIX Collaboration), Phys. Rev. Lett. **107**, 172301 (2011).
[53] J. Pumplin, D. R. Stump, J. Huston, H. L. Lai, P. M. Nadolsky, and W. K. Tung, J. High Energy Phys. 07 (2002) 012.
[54] P. Eden and G. Gustafson, Z. Phys. C **75**, 41 (1997).
[55] J. Adams *et al.* (STAR Collaboration), Phys. Rev. Lett. **97**, 152302 (2006).
[56] I. Arsene *et al.* (BRAHMS Collaboration), Phys. Rev. Lett. **98**, 252001 (2007).
[57] X.-N. Wang, Phys. Rev. C **58**, 2321 (1998).
[58] S. Albino, B. A. Kniehl, and G. Kramer, Nucl. Phys. **B725**, 181 (2005).
[59] O. Adriani *et al.* (LHCf Collaboration), Phys. Rev. D **86**, 092001 (2012).
[60] V. P. Goncalves and M. L. L. da Silva, Nucl. Phys. **A906**, 28 (2013).
[61] O. Adriani, E. Berti, L. Bonechi, M. Bongi, G. Castellini, R. D'Alessandro, M. Del Prete, M. Haguenauer *et al.*, Phys. Rev. C **89**, 065209 (2014).